ASSOCIAZIONE NAZIONALE ITALIANA DI INGEGNERIA SISMICA
ANIDIS
Italian National Association of Earthquake Engineering

XVIII CONVEGNO ANIDIS
L'ingegneria sismica in Italia
ASCOLI PICENO 2019
15-19 Settembre

Novel seismic reliability indexes able to capture epistemic uncertainties

Mariano Angelo Zanini[a], Lorenzo Hofer[a], Flora Faleschini[a,b], Carlo Pellegrino[a]
[a] *Dipartimento di Ingegneria Civile, Edile e Ambientale, Università degli Studi di Padova, Via Marzolo, 35131 Padova, Italy*
[b] *Dipartimento di Ingegneria Industriale, Università degli Studi di Padova, Via Gradenigo 6/A, 35131 Padova, Italy*

Keywords: epistemic uncertainty, fragility analysis, NLTHAs, seismic reliability.

ABSTRACT
The classic approach for computing seismic reliability of a structural system requires a seismic hazard curve and a fragility function and leads to the estimation of the failure probability of the investigated damage state. However, resulting failure probability is strongly related to the preliminary assumptions in both hazard and fragility analyses, and slight changes in the input model parameters may cause relevant variability of seismic reliability estimates. The present work formalizes a general approach to be followed when dealing with seismic reliability assessment of structural systems, aimed at taking into account the whole uncertainties of the input parameters within hazard and fragility models. In the proposed approach, probability of failure becomes in turn a random variable and therefore new indexes are introduced, namely *Expected Failure Rate*, *Failure Rate Dispersion*, *Characteristic Failure Rate*, *Center of Seismic Reliability* and *Characteristic Seismic Reliability*.

1 INTRODUCTION

In seismic reliability analysis, it is of paramount importance to compute failure probability, that is the basic metric of structural safety, i.e. the probability to meet or exceed a target performance level or damage state (ISO 2015). However, failure probability estimates are strongly related to assumed models and input data at both hazard and fragility sides, since both the models themselves and their parameters are uncertain. This issue is mainly due to an incomplete knowledge of such processes (i.e., the so-called epistemic uncertainty). Quantifying the impact of uncertainties in seismic reliability and risk analysis is therefore an emerging challenge that researchers in earthquake engineering are asked to address, since a specific scientific literature is still scarce.

Some uncertainty assessments were carried out in previous research works within the context of seismic hazard analysis, pointing out a clear distinction between aleatory and epistemic uncertainties (Bommer 2003; Rebez and Slejko 2004; Gaspar-Escribano et al. 2015). In the current practice of Probabilistic Seismic Hazard Analysis (PSHA), one of the most widely adopted method for addressing hazard epistemic uncertainty is the so-called logic tree approach (Kularni et al. 1984), in which every node represents a potential source of epistemic uncertainty, and the corresponding outcoming branches represent the possible alternatives. Through the logic tree approach, it is possible to consider both the intra- and the inter-model uncertainties, the former due to uncertainty in the model parameters, the latter for describing the uncertainty among models. Despite its wide adoption in PSHA (Field et al. 2014), the use of logic trees is often debated, due to potential drawbacks (Bommer and Scherbaum 2008).

Some studies were also carried out in order to analyze the impact of finite element (FE) model selection and modelling simplifications (Most 2011; Haukaas and Gardoni 2011; Castaldo et al. 2018), record selection (Sousa et al. 2017; Zanini et al. 2017), and the impact of uncertainty in FE modelling parameters on the seismic fragility estimates (Padgett and DesRoches 2007; Choine et al. 2014).

However, despite the growing attention on such topic, there is a substantial lack of a general approach to be conventionally followed in order to quantify the impact of uncertainties in seismic reliability analysis. As previously reported,

epistemic uncertainties associated to both hazard and fragility were always separately considered in literature studies, without any indication on the prevailing source of randomness when assessing seismic reliability that considers both.

For the abovementioned reasons, the present work illustrates, as main novelty element, a general approach for the seismic reliability assessment, able to investigate the uncertainty of λ_f arising from epistemic uncertainties linked to both hazard and fragility models, based on the formalization of the dependence of $\lambda_f(\boldsymbol{\Theta})$ on model parameters $\boldsymbol{\Theta}$. The proposed general approach allows quantifying the degree of belief that the risk analyst has for a certain seismic reliability estimate, on the basis of the uncertainties' levels existing in the assumption of both hazard and fragility model parameters. As a further novelty element, the paper proposes some new seismic reliability indexes, namely Expected Failure Rate, Failure Rate Dispersion, Characteristic Failure Rate, Center of Seismic Reliability and Characteristic Seismic Reliability, for communicating the failure rate uncertainty and using results of the uncertainty analysis for design/assessment purposes.

2 UNCERTAINTIES IN THE COMPUTATION OF THE FAILURE RATE

In this Section, an overview on the sources of uncertainty linked to both hazard and fragility assessment methods currently in use is provided. In the Performance-Based Earthquake Engineering (PBEE) framework (Cornell and Krawinkler 2000), the occurrence of the main earthquakes at the construction site is commonly assumed to be a Homogenous Poisson Process (HPP). Under this hypothesis, and not considering damage accumulation on structures, the process of events causing the structural failure is also represented by an HPP, whose unique parameter, the failure rate λ_f, can be used for computing the failure probability in any time interval. For this reason, the failure rate λ_f represents one of the most used risk indicators, mainly due to its simplicity and its unique dependence on the seismic hazard and on the structural behavior. It is computed as:

$$\lambda_f = \int_{im} P[f|im] \cdot |d\lambda_{im}| \quad (1)$$

where λ_{im} is the *hazard curve* and represents the seismicity at a specific site, whereas the $P[f|im]$ is the *fragility curve* and it characterizes the probabilistic structural behavior of a structural system (probability of reach and exceed a specific damage level). Current state-of-the-art approaches for the computation of λ_{im} are based on PSHA (Cornell 1968; McHuire 1995), which associates to each ground motion intensity measure $IM = im$ value, the corresponding annual rate of events exceeding im at the site where the structure is located. The most widely adopted intensity measure IM is the peak ground acceleration (PGA), i.e. the spectral acceleration corresponding to a structural period equal to zero; however, for specific applications, spectral accelerations for other different structural period can be used. In Eq. (1) λ_{im}, $|d\lambda_{\mathrm{im}}|$ can be easily obtained as the derivative of the hazard curve:

$$|d\lambda_{\mathrm{im}}| = -\frac{d\lambda_{\mathrm{im}}}{d(im)} d(im) \quad (2)$$

$P[f|im]$ represents the probability of reach and exceed a specific damage level, conditioned on a specific im value. The *fragility curve* $P[f|im]$ is strongly influenced by the type of analyzed structural system, and its calibration is commonly based on results carried out with a set of nonlinear dynamic analyses. Among all procedures proposed in literature for the calibration of $P[f|im]$ parameters, the most used are the Incremental Dynamic Analysis (IDA, Vamvatsikos and Cornell 2004), the Cloud-Analysis (CA, Jalayer and Cornell 2003), and the Multi-Stripes Analysis (MSA, Baker 2015). λ_f computed with Eq. (1) is a point estimate of the failure rate, that derives from specific assumed parameters both in λ_{im} and in $P[f|im]$. In this context, λ_f is thus function of a set of parameters $\boldsymbol{\Theta}$ contained in both the *hazard* ($\boldsymbol{\Theta}_H$) and in the *fragility curve* ($\boldsymbol{\Theta}_F$). When these model parameters $\boldsymbol{\Theta} = [\boldsymbol{\Theta}_H; \boldsymbol{\Theta}_F]$ are assumed to be random variables (RVs), the failure rate itself becomes a RV with unknown distribution and moments.

2.1 Hazard curve uncertainties

The hazard curve λ_{im} is commonly computed via the PSHA integral as:

$$\lambda_{im} = \sum_{i=1}^{n_{SZ}} \upsilon_{m_{min,i}} \int_{m_{min,i}}^{m_{max,i}} \int_{r_{min,i}}^{r_{max,i}} P[IM > im|m,r] f_{M_i}(m) f_{R_i}(r)\, dm\, dr \quad (3)$$

where $\upsilon_{m_{min,i}}$ is the rate of occurrence of earthquakes greater than a suitable minimum magnitude $m_{min,i}$ of the i^{th} seismogenic zone (*SZ*), $f_{M_i}(m)$ is the magnitude distribution for the i^{th} *SZ* and $f_{R_i}(r)$ is the distribution of the source i^{th}-to-site distance. Finally, $P[IM > im|m,r]$ represents the probability to exceed the value im at the site of interest due to a seismic event with magnitude m occurring at a certain epicenter-to-site distance r. $P[IM > im|m,r]$ is usually computed with a Ground Motion Prediction Equation (GMPE), which predicts the probability distribution of an *IM* of interest as a function of many input variables, like magnitude, source-to-site distance, soil type, faulting style. Model parameters to be treated as RVs can be found involved in the hazard computation, in all the above terms. When a truncated Gutenberg–Richter (G-R) occurrence law (Gutenberg and Richter 1944) is adopted for the i^{th} *SZ*, the magnitude distribution $f_{M_i}(m;\boldsymbol{\Theta}_M)$ depends on the parameters vector $\boldsymbol{\Theta}_M = [M_{max,i}, M_{min,i}, B_i]$, where $M_{max,i}$ and $M_{min,i}$ represent the magnitude interval of events that can occur in *SZ*, and B_i represent the slope of the G-R relationship. Also $\gamma_{M_{min,i}}$ of Eq. (3) can be considered as random and it is included among model parameters $\boldsymbol{\Theta}_M$ related to the G-R law. Similarly to $f_{M_i}(m;\boldsymbol{\Theta}_M)$, also $f_{R_i}(r;\boldsymbol{\Theta}_R)$ could be characterized by random parameters $\boldsymbol{\Theta}_R$, e.g. the fault length, in case that a linear source model is assumed, the fault diameter, for a circular *SZ*, or the fault depth. Finally, the term $P[IM > im|m,r;\boldsymbol{\Theta}_{GMPE}]$ depends on the GMPE regression coefficients involved to compute the distribution parameters of the im expected in the specific site. Usually $\boldsymbol{\Theta}_{GMPE}$ includes a factor representing the soil type, the style of faulting, or other regression coefficients. Considering all the possible uncertainty sources involved in the hazard curve computation, Eq. (3) can be rewritten as:

$$\lambda_{im}(\boldsymbol{\Theta}_{\mathrm{H}}) = \sum_{i=1}^{n_{SZ}} \gamma_{M_{min,i}} \int_{M_{min,i}}^{M_{max,i}} \int_{R_{min,i}}^{R_{max,i}} P[IM > im|m,r;\boldsymbol{\Theta}_{GMPE}] f_{M_i}(m;\boldsymbol{\Theta}_M) f_{R_i}(r;\boldsymbol{\Theta}_R)\, dm\, dr \qquad (4)$$

Note the general form of this notation, which allows including also the epistemic uncertainty related to the adoption of different GMPEs or different earthquake occurrence models, by simply introducing a *probability mass function* weighting each possible alternative. In this way, the classical *logic tree approach* (Kulkarni et al. 1984) is included in the proposed formulation.

2.2 Fragility curve uncertainties

The fragility function $P[f|im]$ is usually derived from results of nonlinear dynamic analysis performed with specific structural software. Simulations are needed for obtaining a sample of structural responses for a given set of selected ground motions. Structural responses are usually quantified by setting an engineering demand parameter (EDP) of interest, i.e. a metric that can be used to estimate damage to structural (and/or non-structural) components. Common EDPs may be the inter-story drift, the pier-top displacement etc. Such data are further used to calibrate the relationship between the ground shaking level and the EDP of interest, i.e. the Probabilistic Seismic Demand Model (PSDM), able to capture non-linear seismic behavior of a structural system for increasing ground shaking levels (Bazzurro et al. 1998). Consequently, only an estimate of the fragility curve is obtained, since it is expected to change when varying the input ground motions sample. Several procedures can be found in literature for estimating the fragility parameters from structural analysis, among all the most adopted ones are the *IM-based* Incremental Dynamic Analysis (IDA) approach and the Cloud analysis approach.

In the first case, a set of *n* IDA curves, are used for drawing a sample of *n* intensity measures $[im_1, im_2, \ldots, im_n]$, at which the structural response reaches a specific undesired threshold level $\overline{edp}$ of engineering demand parameter (EDP). Each im_i can be seen as a realization of the random variable IM_f, i.e. of ground motion intensities that cause the reaching of the investigated structural damage level. Thus, the structural fragility can be computed as the probability of the RV IM_f to do not exceed the specific im value. In the case that the RV $ln(IM_f)$ is normally distributed, as commonly assumed in most of PBEE applications and widely proved in literature (Ibarra and Krawinkler 2005), $\mu_{ln(IM_f)}$ and $\sigma_{ln(IM_f)}$ represent respectively the mean and the standard deviation of $ln(IM_f)$ distribution. When these two parameters are treated as RVs, the following equation for the structural fragility can be derived

$$P[f|im;\boldsymbol{\Theta}_F] = P\left[IM_f \le im;\boldsymbol{\Theta}_F\right] = \Phi\left[\frac{ln(im)-\mu_{ln(IM_f)}}{\sigma_{ln(IM_f)}}\right] \quad \text{with} \quad \boldsymbol{\Theta}_F = \left[\mathrm{M}_{ln(IM_f)}, \Sigma_{ln(IM_f)}\right] \tag{5}$$

From a sample $[im_1, im_2, \dots, im_n]$ of *n* ground motion values, obtained with structural analysis, it is possible to derive a point estimate of $\mathrm{M}_{ln(IM_f)}$ and $\Sigma_{ln(IM_f)}$ as:

$$\hat{\mu}_{ln(IM_f)} = \frac{1}{n}\sum_{i=1}^{n} ln(im_i) \tag{6}$$

$$\hat{\sigma}_{ln(IM_f)}{}^2 = \frac{1}{n-1}\sum_{i=1}^{n}\left[ln(im_i) - \hat{\mu}_{ln(IM_f)}\right]^2 \tag{7}$$

and thus, a point estimate $P\left[f\middle|im;\widehat{\boldsymbol{\Theta}}_F\right]$ of the fragility function $P[f|im;\boldsymbol{\Theta}_F]$:

Furthermore, an approximated value for the variance of the mean $\hat{\mu}_{ln(IM_f)}$ and variance $\hat{\sigma}_{ln(IM_f)}{}^2$ estimator, can be computed as:

$$VAR\left[\hat{\mu}_{ln(IM_f)}\right] \approx \frac{\hat{\sigma}_{ln(IM_f)}{}^2}{n} \tag{8}$$

$$VAR\left[\hat{\sigma}_{ln(IM_f)}{}^2\right] \approx \frac{2\cdot\hat{\sigma}_{ln(IM_f)}{}^4}{n-1} \tag{9}$$

Regarding the Cloud Analysis approach, similar considerations on the model parameters can be done. In this case, the fragility computation takes origin from a sample of *n* ground motions intensities $[im_1, im_2, \dots, im_n]$ and the corresponding sample of structural responses $[edp_1, edp_2, \dots, edp_n]$. In this case, the fragility function assumes the following form [50]:

$$P[f|im] = P\left[EDP > \overline{edp}|im\right] = 1 - P\left[EDP \le \overline{edp}|im\right] = 1 - \Phi\left[\frac{ln(\overline{edp})-ln(edp)}{\beta}\right] \tag{10}$$

In Eq. (10), $\overline{edp}$ is the median value of the assumed structural limit state, and edp represents the median estimate of the demand that can be computed with a ln-linear regression model as:

$$ln(edp) = a_1 + a_2 \cdot ln(im) \tag{11}$$

Finally, β is the standard deviation of the demand conditioned on im and can be estimated from the regression of the seismic demands as

$$\beta = \sqrt{\frac{\sum_{i=i}^{n}\left[ln(edp_i)-(a+b\cdot ln(im_i))\right]^2}{n-2}} \tag{12}$$

Note that this model assumes a deterministic capacity, and consequently with a standard deviation equal to 0. When treating a_1, a_2 and β as RVs, the fragility itself becomes random and Eq. (13) can be rewritten as:

$$P[f|im;\boldsymbol{\Theta}_F] = 1 - \Phi\left[\frac{ln(\overline{edp})-ln(a_1+a_2\cdot ln(im))}{\beta}\right] \quad \text{with } \boldsymbol{\Theta}_F = [A_1, A_2, \mathrm{B}\,] \tag{13}$$

Parameters$a$, b and β are commonly estimates from *n* couples of points $[ln(im_i), ln(edp_i)]$ obtained from structural analysis, and thus it makes the structural fragility itself an estimate $P\left[f\middle|im;\widehat{\boldsymbol{\Theta}}_F\right]$. Finally, since the estimates of A_1, A_2 and B are computed with a linear regression, the moments of these three estimators are known and are provided by the following equations:

$$VAR[\hat{a}_1] \approx \left(\frac{1}{n} + \frac{\hat{m}^2}{\sum_{i=1}^{n}[log(im_i)-\hat{m}]^2}\right)\cdot\hat{\beta}^2 \tag{14}$$

$$VAR[\hat{a}_2] \approx \frac{\hat{\beta}^2}{\sum_{i=1}^{n}[log(im_i)-\hat{m}]^2} \tag{15}$$

$$COV[\hat{a}_1, \hat{a}_2] \approx \frac{-\hat{m}\cdot\hat{\beta}^2}{\sum_{i=1}^{n}[log(im_i)-\hat{m}]^2} \tag{16}$$

$$VAR\left[\hat{\beta}^2\right] \approx \frac{2\cdot\hat{\beta}^4}{n-2} \tag{17}$$

where $\hat{m} = \frac{1}{n}\sum_{i=1}^{n} log(im_i)$, i.e. the mean of the im_i values of the records used for the structural analysis.

3 PROPOSED NEW SEISMIC RELIABILITY INDEXES

This Section formalizes the dependence of $\lambda_f(\boldsymbol{\Theta})$ on model parameters and illustrates the newly proposed seismic reliability indexes. As widely shown in the previous sections, the failure rate λ_f is function of series of uncertain parameters that are involved in both the hazard and fragility computation. As a consequence, Eq. (1) can be re-written in a more general way, as:

$$\lambda_f(\boldsymbol{\Theta}) = \int_{im} P[f|im;\boldsymbol{\Theta_F}] \cdot |d\lambda_{\mathrm{im}};\boldsymbol{\Theta_H}| \qquad (18)$$

for highlighting the randomness of the failure rate itself, and its dependence on the two uncertainty sources.

In the most general case, the expected value of the seismic failure rate $E[\lambda_f(\boldsymbol{\Theta})]_{HF}$ is provided by the following equation:

$$E[\lambda_f(\boldsymbol{\Theta})]_{HF} = \int \lambda_f(\boldsymbol{\Theta}) f(\boldsymbol{\Theta}) d\boldsymbol{\Theta} = \int \left\{ \int_{im} P[f|im;\boldsymbol{\Theta_F}] \cdot |d\lambda_{im};\boldsymbol{\Theta_H}| \right\} f(\boldsymbol{\Theta}) d\boldsymbol{\Theta} \qquad (19)$$

Since most of times $\boldsymbol{\Theta}$ is a vector composed by several parameters, and, its mathematical form of $\lambda_{im}$is not *a-priori* known, the computation of Eqs. (20-22) can be difficult in a close analytical way. For this reason, suitable simulation methods, as the Monte Carlo Simulation (MCS), are required. In this case, the result accuracy is important, and may be measured and checked, by setting a suitable threshold value for the coefficient of variation (C.O.V.) of the solution. This procedure allows obtaining an adequate number of $\lambda_{f.i}$ samples, and thus drawing the (*pdf*) of the failure rate $f_{\Lambda_f}(\lambda_f)$, by fitting the samples with a suitable known function.

The failure rate distribution $f_{\Lambda_f}(\lambda_f)$ represents the most complete information on the seismic reliability of a structural system, and starting from this, new seismic reliability indexes are defined in order to provide a clear and synthetic description of the seismic reliability and its accuracy. First, the *Expected Failure Rate* μ_{Λ_f} representing the weighted average of the Λ_f RV, can be derived as:

$$\mu_{\Lambda_f} = E[\Lambda_f] = \int \lambda_f \cdot f_{\Lambda_f}(\lambda_f) d\lambda_f \qquad (20)$$

Then *Failure Rate Dispersion* δ_{Λ_f} can be computed as a measure of the degree of dispersion of the failure rate distribution, derived as the coefficient of variation of Λ_f. This indicator is preferred to the common variance (or standard deviation) since the measure of variability is more meaningful if measured relative to the central value, and μ_{Λ_f} is always positive:

$$\delta_{\Lambda_f} = \frac{\sigma_{\Lambda_f}}{\mu_{\Lambda_f}} = \frac{\sqrt{\int (\lambda_f - \mu_{\Lambda_f})^2 \cdot f_{\Lambda_f}(\lambda_f) d\lambda_f}}{\int \lambda_f \cdot f_{\Lambda_f}(\lambda_f) d\lambda_f} \qquad (21)$$

Hence, in analogy with the philosophy of semi-probabilistic structural safety approach, the *Characteristic Failure Rate* $\lambda_{f,k}$ is introduced as the failure rate value, whose probability of being exceeded is 5%, and computed as:

$$\lambda_{f,k} = F_{\Lambda_f}^{-1}(0.95) \qquad (22)$$

where $F_{\Lambda_f}^{-1}(0.95)$ is the inverse of the cumulative density function CDF of the RV Λ_f.

Finally, in order to allow a direct comparison with target structural safety values provided in the current technical codes for constructions, other two new seismic reliability indexes are introduced using the actual metric for reliability analysis, namely *Center of Seismic Reliability* $\beta_{E,\mu,t}$ and *Characteristic Seismic Reliability* $\beta_{E,k,t}$ indexes, computed respectively as follows:

$$\beta_{E,\mu,t} = -\Phi^{-1}(1 - e^{-\mu_{\Lambda_f} t}) \qquad (23)$$

$$\beta_{E,k,t} = -\Phi^{-1}(1 - e^{-\lambda_{f,k} t}) \qquad (24)$$

where *t* is the target time window of interest and the subscript "*E*" stands for "earthquake". The final seismic safety check, that needs to be performed in order to confirm the seismic reliability of a structural system, can be expressed as:

$$\beta_{E,k,t} \geq \beta_{target} \qquad (25)$$

where β_{target} represents the target structural reliability to be fulfilled during the time window of interest.

4 CASE-STUDY APPLICATION

The proposed general approach has been applied to an existing single-span open-spandrel RC arch bridge located in the Vicenza district (lat. 46.01, lon. 11.63), northeastern Italy. Five RC arches of 60 m span, 5.5 m arch rise and a transversal spacing of 3 m, each one with a rectangular section of 1 m height and 0.5 m width, characterize the bridge. RC arches are connected with RC arch transverse beams placed at the arches axes with a longitudinal spacing of 6 m, and a

rectangular section of 0.3 m height and 0.6 m width. RC piers, with a square section of 0.3 m side and placed on each RC arch with a longitudinal spacing of 6 m, sustain the girder composed by a grillage of RC beams. In particular, longitudinal deck RC beams are characterized by a rectangular section of 0.5 m height and 0.3 m width, whereas transversal beams are realized with a rectangular section of 0.4 m height and 0.3 m width. The RC beam grillage supports a 0.2 m thickness RC slab constituting the roadway surface, and bounded with marble parapets. Figure 1 shows main geometrical features, i.e. elevation, and longitudinal and transversal sections of the analyzed RC arch bridge.

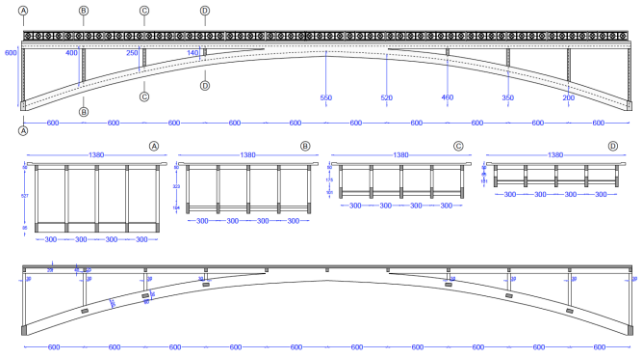

Fig. 1: RC arch bridge: elevation, transversal and longitudinal sections.

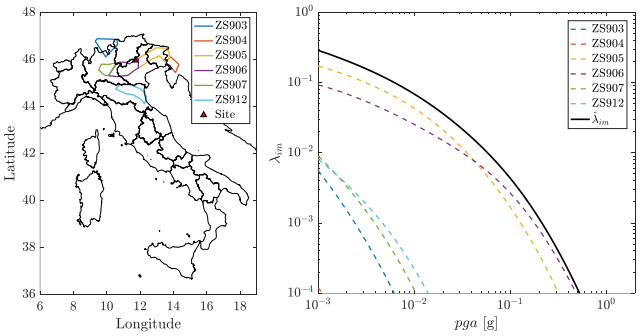

Fig. 2: Bridge site, adopted seismogenic source model and PSHA results.

For the classic seismic reliability assessment, a PSHA and a seismic fragility analysis have been conducted. The seismogenic source zone model ZS9 detailed in Meletti et al. (2008) has been adopted, using Gutenberg-Richter (G-R) recurrence laws for each of the six SZs considered (i.e. SZs # 903, # 904, # 905, # 906, # 907 and # 912). Main G-R parameters (i.e., mean annual rate of events with magnitude above the minimum magnitude value $\nu_{m_{min,i}}$, slope coefficient b, minimum magnitude value m_{min} and maximum magnitude value m_{max}) as reported in Barani et al. (2009) with Gaussian distributions with C.O.V.s of 0.1 for all parameters except to m_{min} with C.O.V. equal to 0.01. As regards the ground motion prediction equation (GMPE) model, the formulation proposed by Bindi et al. (2011) has been adopted, considering a type-B soil class (V_{S30} = 360 – 800 m/s) on the basis of available information on the local stratigraphy. Figure 2 maps the bridge site with respect to the six SZs considered, and the resulting seismic hazard curve, highlighting how SZs # 905 and # 906 mostly contribute to the hazard of the bridge site.

Seismic fragility analysis has been conducted performing a set of non-linear time history analyses (NLTHAs) on a 3-D finite element (FE) model of the analyzed RC arch bridge. The 3-D FE model has been implemented in Seismostruct software platform (Seismosoft 2013) in order to properly characterize main structural features of the analyzed bridge for the following seismic reliability analysis purposes. In particular, frame elements (i.e. arches, piers and arch transverse beams) have been modelled using distributed plasticity fiber-section elements with force-based formulation, whereas deck RC grillage beams (both longitudinal and transversal) have been modelled as elastic elements. Deck RC grillage beams are connected through rigid links to the RC slab, which is realized with a rigid diaphragm constraint type. Figure 3 shows a 3-D view of the FE model of the RC arch bridge, with information on longitudinal reinforcement and stirrups in each structural element, discretization of fiber cross-sections for non-linear RC elements, and adopted constitutive laws for unconfined and confined concrete and steel reinforcement bars.

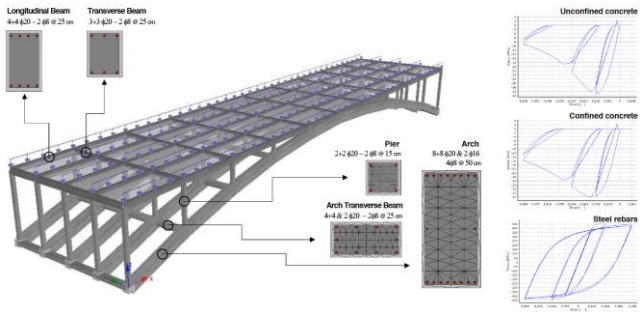

Fig. 3: RC arch bridge FE model, with adopted constitutive laws for unconfined - confined concrete and steel rebars.

A set of 30 natural 3-D seismic records has been collected from the European Strong Motion Database (Luzi et al. 2016), and further used to execute the NLTHAs. NLTHAs have been subsequently run, extracting 3-D interstory drift

ratios time histories, and thus deriving the maximum IDR value of the first external RC pier with 6 m height for each record. Cloud analysis method has been then used to derive the seismic fragility curves of the analyzed RC arch bridge, expressed in terms of horizontal PGA. Results derived from NLTHAs have been fitted in the bi-logarithmic plane according to Eq. (11), thus deriving $\hat{a}_1$ and $\hat{a}_2$ coefficient of the ln-linear regression model and the standard deviation $\hat{\beta}^2$ via Eq. (12), and equal to -3.979, 1.055 and 0.42, respectively. Four different damage states (i.e. Slight, Moderate, Extensive and Complete Damage) has been fixed considering IDR thresholds equal to 0.25%, 0.5%, 1% and 2% respectively, thus leading to derive four fragility curves computed with Eq. (10). Figure 4 shows the results of Cloud Analysis with NLTHA data points, the assumed IDR thresholds and resulting set of fragility curves.

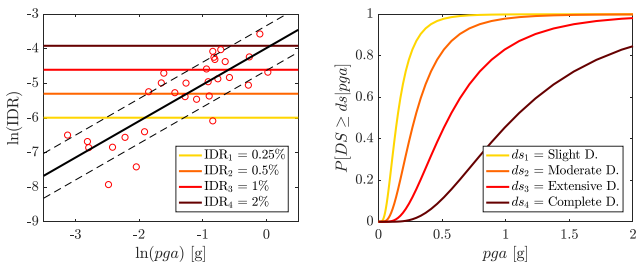

Fig. 4: Cloud analysis results and related analytical fragility curves.

MCS technique has been then used to compute an adequate number of failure rate samples $\lambda_{f,i}$, setting an adequate and high accuracy level, ensured by the fulfilment of a C.O.V. of the solution smaller than to 2%. Figure 5 shows resulting hazard and fragility samples as well as the distribution of failure rates.

Once the failure rate *pdf* $f_{\Lambda_f}(\lambda_f)$ has been fitted, the last step consists in the computation of the new seismic reliability indexes, according to Eqs. (21-24). First, the *Expected Failure Rate* μ_{Λ_f} has been derived with value equal to 5.70E-05, slightly higher than the benchmark case represented by the point estimate $\hat{\lambda}_f$ = 4.89E-05. *Failure Rate Dispersion* δ_{Λ_f} has been then computed, resulting in an estimate equal to 0.659. Hence, the *Characteristic Failure Rate* $\lambda_{f,k}$ (i.e. the failure rate value whose probability of being exceeded is 5%) has been calculated, leading to a value equal to 1.29E-04. It is worth noting how the ratio $\lambda_{f,k}/\hat{\lambda}_f$ between the *Characteristic Failure Rate* $\lambda_{f,k}$ and the point estimate of the seismic failure rate derived with the classic approach $\hat{\lambda}_f$ is equal to 2.65, respectively, thus evidencing how in the specific case $\lambda_{f,k}$ has values larger than twice of the $\hat{\lambda}_f$ point estimate derived with the current classic seismic reliability assessment approach.

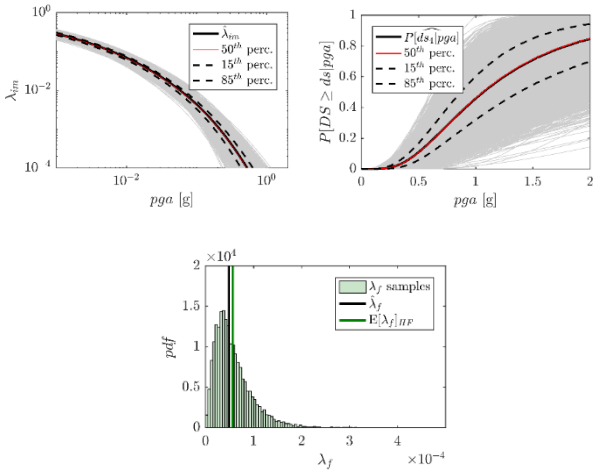

Fig. 5: Failure rate samples $\lambda_{f,i}$ obtained considering hazard and fragility uncertainties.

On those bases, the final seismic reliability indexes *Center of Seismic Reliability* $\beta_{E,\mu,t}$ and *Characteristic Seismic Reliability* $\beta_{E,k,t}$ have been derived according to Eqs. (23-24), considering a 1-year target time window, and resulting in $\beta_{E,\mu,1}$ values equal to 3.859 and $\beta_{E,k,1}$ estimate of 3.654, respectively. Lastly, considering a yearly target structural reliability $\beta_{target,1}$ equal to 4.7 (European Committee for Standardization, 2002) for the Ultimate Limit State, the structural safety assessment carried out with Eq. (28) is not fulfilled, thus requiring further efforts in designing a seismic retrofit project for the analysed RC arch bridge structure.

5 CONCLUSIONS

The present work illustrated a novel general approach for the assessment of seismic reliability of structural systems able to account for underlying uncertainties in the definition of the input parameters of seismic hazard and fragility models. This study showed how the use of the classic approach for computing seismic reliability leads to a point estimate of the failure probability

for a DS of interest, without knowledge of the level of uncertainty characterizing it. A set of new seismic reliability indexes was therefore defined, namely *Expected Failure Rate*, *Failure Rate Dispersion*, *Characteristic Failure Rate*, *Center of Seismic Reliability* and *Characteristic Seismic Reliability*.

REFERENCES

Baker J.W. (2015) Efficient analytical fragility function fitting using dynamic structural analysis. Earthquake Spectra, 31(1):579–599.

Barani S., Spallarossa D., Bazzurro P. (2009) Disaggregation of probabilistic ground motion hazard in Italy. Bulletin of the Seismological Society of America, 99: 2638-2661.

Bazzurro P., Cornell C.A., Shome N., Carballo J.E. (1998) Three proposals for characterizing MDOF nonlinear seismic response. Journal of Structural Engineering, 124(11): 1281-1289.

Bindi D., Pacor F., Luzi L., Puglia R., Massa M., Ameri G., Paolucci R. (2011) Ground motion prediction equations derived from the Italian strong motion database, Bulletin of Earthquake Engineering, 9: 1899–1920.

Bommer J.J. (2003) Uncertainty about the uncertainty in seismic hazard analysis, Engineering Geology, 70(1-2): 165-168.

Bommer, J. J., and Scherbaum, F. (2008) The use and misuse of logic-trees in probabilistic seismic hazard analysis, Earthquake Spectra 24, 997–1009.

Castaldo P., Gino D., Bertagnoli G., Mancini G. (2018) Partial safety factor for resistance model uncertainties in 2D non-linear finite element analysis of reinforced concrete structures, Engineering Structures, 176:746-762.

Choine M.N., O'Connor A., Padgett J.E. (2014) Comparison between the seismic performance of integral and jointed concrete bridges, Journal of Earthquake Engineering, 19(1): 172-191

Cornell C. (1968) Engineering seismic risk analysis. Bulletin of Seismological Society of America, 58(5): 1583-1606.

Cornell C.A., Krawinkler H. (2000) Progress and challenges in seismic performance assessment. PEER Centre News, 3(2): 1-3.

European Committee for Standardization (2002) Eurocode 0: Basis of structural design. Technical Committee CEN/TC 250 "Structural Eurocodes", pp. 90.

Field, E.H., Arrowsmith, R.J., Biasi, G.P., Bird, P., Dawson, T.E., Felzer, K.R., Jackson, D.D., Johnson, K.M., Jordan, T.H., Madden, C., Michael, A.J., Milner, K.R., Page, M.T., Parsons, T., Powers, P.M., Shaw, B.E., Thatcher, W.R., Weldon II, R.J., Zeng, Y. (2014) Uniform California Earthquake Rupture Forecast, Version 3 (UCERF3)-The Time-Independent Model. Bulletin of the Seismological Society of America, 104 (3): 1122–1180.

Gaspar-Escribano J.M., Rivas-Medina A., Parra H., Cabanas L., Benito B., Ruiz Barajas S., Martinez Solares J.M. (2015) Uncertainty assessment for the seismic hazard map of Spain, Engineering Geology, 199: 62-73.

Gutenberg B., Richter, C.F. (1944) Frequency of earthquakes in California, Bulletin of the Seismological Society of America, 34(4), 185-188.

Haukaas T., Gardoni P. (2011) Model uncertainty in finite-element analysis: Bayesian finite elements, Journal of Engineering Mechanics, 137(8): 519–526.

Ibarra L.F., Krawinkler H. (2005) Global collapse of frame structures under seismic excitations. John A. Blume Earthquake Engineering Center, Stanford, CA, 324.

International Organization for Standardization (ISO) (2015) ISO 2394, General Principles on Reliability for Structures. Switzerland.

Jalayer F., Cornell C.A. (2003) Direct probabilistic seismic analysis: implementing non-linear dynamic assessments. Stanford University.

Kulkarni, R.B., Youngs, R.R., Coppersmith, K.J. (1984) Assessment of confidence intervals for results of seismic hazard analysis. Proceedings of the Eighth World Conference on Earthquake Engineering, San Francisco, Vol. 1, 263–270.

Luzi L., Puglia R., Russo E. & ORFEUS WG5 (2016) Engineering Strong Motion Database, version 1.0. Istituto Nazionale di Geofisica e Vulcanologia, Observatories & Research Facilities for European Seismology. doi: 10.13127/ESM. Available at: https:// http://esm.mi.ingv.it/.

McGuire R.K. (1995) Probabilistic seismic hazard analysis and design earthquakes: closing the loop. Bull Seismol Soc Am.;85(5):1275-1284.

Meletti C., Galadini F., Valensise G. (2008) A seismic source zone model for the seismic hazard assessment of the Italian territory. Tectonophysics, 450: 85–108.

Most T. (2011) Assessment of structural simulation models by estimating uncertainties due to model selection and model simplification, Computer and Structures, 89(17–18): 1664–72.

Padgett J.E., DesRoches R. (2007) Sensitivity of seismic response and fragility to parameter uncertainty, Journal of Structural Engineering, 133(12): 1710-1718.

Rebez A., Slejko D. (2004) Introducing epistemic uncertainties into seismic hazard assessment for the broader Vittorio Veneto area, Bollettino di Geofisica Teorica ed Applicata, 45(4): 305-320.

SeismoSoft (2013) SeismoStruct – a computer program for static and dynamic nonlinear analysis of frames structures. Available at: http://www.seismosoft.com.

Sousa L., Marques M., Silva V., Varum H. (2017) Hazard disaggregation and record selection for fragility analysis and earthquake loss estimation, Earthquake Spectra, 33(2): 529-549.

Vamvatsikos D., Cornell C.A. (2004) Applied incremental dynamic analysis. Earthquake Spectra, 20(2):523–553.

Zanini M.A., Hofer L., Faleschini F., Pellegrino C. (2017) The influence of record selection in assessing uncertainty of failure rates, Ingegneria Sismica, 34(4): 30-40.